

Incorporation of Rare-Earth Complex $\text{Eu}(\text{TTA})_4\text{C}_5\text{H}_5\text{NC}_{16}\text{H}_{33}$ into Surface-Modified Si–MCM-41 and Its Photophysical Properties

Qinghong Xu,[†] Liansheng Li,[†] Xinsheng Liu,[‡] and Ruren Xu^{*,†}

Key Laboratory of Inorganic Synthesis & Preparative Chemistry, Jilin University, Changchun 130023, People's Republic of China, and Engelhard Corporation Research and Development, Iselin, New Jersey 08830-0770

Received March 15, 2001. Revised Manuscript Received November 28, 2001

The incorporation of the rare-earth complex $[\text{C}_5\text{H}_5\text{NC}_{16}\text{H}_{33}][\text{Eu}(\text{TTA})_4]$ into surface-modified mesoporous molecular sieve Si–MCM-41 via reactions of the surface Si–OH with different silylation agents such as $(\text{C}_2\text{H}_5\text{O})_3\text{Si}(\text{CH}_2)_2\text{NH}(\text{CH}_2)_2\text{NH}_2$ (NSED), $(\text{C}_2\text{H}_5\text{O})_3\text{Si}(\text{CH}_2)_3\text{NH}_2$ (APTES), and $(\text{C}_2\text{H}_5\text{O})_3\text{Si}(\text{CH}_2)_3\text{CN}$ (TSBT) and their photophysical properties were studied. The results show that the surface silylation of Si–MCM-41 provides a unique chemical environment for the incorporated $[\text{C}_5\text{H}_5\text{NC}_{16}\text{H}_{33}][\text{Eu}(\text{TTA})_4]$ complex. Hydrogen-bonding interactions of the rare-earth complex with its surrounding silylating agents alter the photophysical properties of the rare-earth complex. The emission intensity and color purity of the excited rare-earth complex in these surface-silylated Si–MCM-41 materials increase in the order of Si–MCM-41 < TBST–Si–MCM-41 < APTES–Si–MCM-41 < NSED–Si–MCM-41. Because of the strongest hydrogen bonding in NSED–Si–MCM-41, the rare-earth complex only emits light with a single wavelength, corresponding to ${}^5\text{D}_0\text{--}{}^7\text{F}_2$. This phenomenon is rarely seen in the luminescence of rare-earth complexes. The UV stability and lifetime of Eu^{3+} in the rare-earth complex were also studied, and the results show that the incorporated rare-earth complex exhibits higher UV stability and increased lifetime compared to the pure rare-earth complex.

Introduction

Rare-earth ions and their complexes have characteristic luminescence properties and are widely used in lasers and luminescent materials and as probe ions in microporous and biological materials.^{1,2} In the past, studies on the encapsulation of rare-earth complexes into substrates or matrixes and on guest–host interactions were mainly focused on Langmuir–Blodgett films,³ sol–gel materials,⁴ adsorption on SiO_2 ,⁵ supramolecules,⁶ and some porous materials,^{7,8} while studies on the encapsulation of rare-earth complexes into molecular sieves and on their luminescence properties were reported only very recently. The paper by Rose et al.⁶ in 1997 reported the encapsulation and luminescence properties of $[\text{Eu}(\text{bpy})_2]^{3+}$ in zeolite Y.

The discovery of the mesoporous material MCM-41^{9,10} by Mobil in 1992 opened a new field for material science.^{11–15} As a host material, studies of the encapsulation and assembly of guest molecules in the mesoporous channels have been very extensive.^{16–21} However, there are few reports on the encapsulation of rare-earth complexes into this kind of material and their photophysical properties.^{22,23} It is, therefore, of impor-

* To whom correspondence should be addressed. Fax: +86-431-5671974. E-mail: rrxu@mail.jlu.edu.cn.

[†] Jilin University.

[‡] Engelhard Corporation Research and Development.

(1) Blasse, G.; Grabmaier, B. C. *Luminescent Materials*; Springer-Verlag: Berlin, 1994.

(2) Suib, S. L. In *CRC Photochemistry and Photophysics*; Rabek, J. F., Ed.; CRC Press: Boston, 1991; Vol. III, p 1.

(3) Serra, O. A.; Rosa, I. L. V.; Medeiros, C. L.; Elizabete, M. D.; Zaniquelli, J. *Lumin.* **1994**, *61* and *62*, 112.

(4) Matthews, L. R.; Knobbe, E. T. *Chem. Mater.* **1993**, *5*, 1697.

(5) Hazenkamp, M. F.; Blasse, G. *J. Phys. Chem.* **1991**, *95*, 783.

(6) Rose, I. L. V.; Serra, O. A.; Nassa, E. J. *J. Lumin.* **1997**, *72*, 532.

(7) Hazenkamp, M. F.; van der Veen, A. M. H.; Feiken, N.; Blasse, G. *J. Chem. Soc., Faraday Tran.* **1992**, *88*, 141.

(8) Kresge, C. T.; Leonowicz, M. E.; Roth, W. J.; Vartuli, J. C.; Beck, J. S. *Nature* **1992**, *359*, 710.

(9) Beck, J. S.; Vartuli, J. C.; Roth, W. J.; Leonowicz, M. E.; Kresge, C. T.; Schmitt, K. D.; Chu, C. T.-W.; Olson, D. H.; Sheppard, E. W.; Nccullen, S. B.; Higgins, J. B.; Schlenker, J. L. *J. Am. Chem. Soc.* **1992**, *114*, 10834.

(10) Thomas, J. M. *Nature* **1994**, *368*, 289.

(11) Tanev, P. T.; Chibwe, M. T.; Pinnavaia, J. *Nature* **1994**, *368*, 322.

(12) Schmidt, R.; Stocker, M.; Hansen, E.; Akporiaye, D.; Ellestad, O. H.; *Microporous Mater.* **1995**, *3*, 443.

(13) Wu, C. G.; Bein, T. *Chem. Mater.* **1994**, *6*, 1109. Wu, C. G.; Bein, T. *Science* **1994**, *264*, 1757.

(14) Corma, A.; Fornes, V.; Garcia, H.; Miranda, M. A.; Sabater, M. J. *J. Am. Chem. Soc.* **1994**, *116*, 9767.

(15) Wark, M.; Ortham, A.; Gandschow, M.; Schulz-Ekloff, G.; Woehrl, D. *Ber. Bunsen-Ges.* **1998**, *102*, 1548.

(16) Yamashita, H.; Tanaka, A.; Nishimura, M.; Koyano, K.; Tatsmi, T.; Anpo, M. *Stud. Surf. Sci. Catal.* **1998**, *117*, 551.

(17) Maria, L. C.; Frances, L. C.; Garcia, H.; Marti, V.; Scaiano, J. C. *J. Phys. Chem.* **1996**, *100*, 18152.

(18) Diaz, J. F.; Bedioui, F.; Briot, E.; Devynck, J.; Bulkus, K. J. *J. Microporous Mater.* **1996**, *4*, 89.

(19) O'Brien, S.; Tudor, J.; Low, S. B.; Drewitt, J. M.; Heyes, J. S.; O'Hare, D. *Chem. Commun.* **1997**, *6*, 641.

(20) Ernst, S.; Glaser, R.; Selle, M. *Stud. Surf. Sci. Catal.* **1997**, *105B*, 1021.

(21) Chen, C. Y.; Li, H. X.; Davis, M. E. *Microporous Mater.* **1993**, *2*, 17.

(22) Xu, Q. H.; Li, L. S.; Li, B.; Yu, J. H.; Xu, R. R. *Microporous Mesoporous Mater.* **2000**, *38*, 351–358.

tance to study this system and to shed some light on the understanding of the interactions of the guest with the host and the effects of the interactions on the photophysical properties of the rare-earth complexes.

It is well-known that surface of Si-MCM-41 is covered with OH groups^{9,21} and that OH groups have strong quenching properties toward luminescence of rare-earth complexes.⁷ In the present paper, we report the results of our studies on the modification of the surface of Si-MCM-41 with three kinds of silylating agents, incorporation of a rare-earth complex, [C₅H₅NC₁₆H₃₃][Eu(TTA)₄], into the modified Si-MCM-41, and photophysical properties of these materials using a combination of techniques such as X-ray diffraction (XRD), magic angle spinning nuclear magnetic resonance (MAS NMR), X-ray photoelectron spectroscopy (XPS), UV-vis spectroscopy, SPEX Fluorolog-2T2 spectrofluorometry, and SPEX 1934D phosphorimetry. The stability of the complex in the materials was also studied.

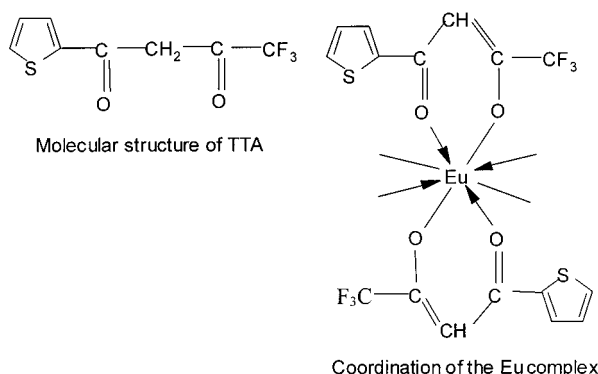
Experimental Section

Chemicals. *N*-[3-(Triethoxysilyl)ethyl]ethylenediamine (NSED; AR), 3-(aminopropyl)triethoxysilane (APTES; AR), and 4-(triethoxysilyl)butyronitrile (TSBT; AR) were purchased from Aldrich, Milwaukee, WI. 2-Thenoyltrifluoroacetone (TTA) is a Fluka reagent. [C₅H₅NC₁₆H₃₃][Eu(TTA)₄] was prepared in our laboratory with a purity of >99%.

Synthesis of Si-MCM-41. The synthesis of Si-MCM-41 accords to the ref 24.

Silylation of Si-MCM-41. Three silylation agents, NSED, APTES, and TSBT, were used for this purpose. Three 0.1 g calcined Si-MCM-41 samples were mixed respectively with these silylation agents and stirred at room temperature for 12, 16, and 16 h. The solids were separated by filtration, washed thoroughly with chloroform and dichloromethane, and then dried at room temperature. For the silylation, the use of APTES as the silylation agent has been reported in the literature.²⁵

Synthesis of [C₅H₅NC₁₆H₃₃][Eu(TTA)₄].^{26,27} Under stirring, 0.888 g of HTTA was added to a hot solution of 0.403 g of C₅H₅NC₁₆H₃₃Br·H₂O in 25 mL of alcohol; after it was dissolved, 5 mL of a 0.77 M NaOH solution and 0.258 g of a EuCl₃ alcohol solution were dropped into the solution. The mixture was refluxed for 1 h, then cooled, filtered, and recrystallized in alcohol, and then dried over P₂O₅. The TTA structural formula and its coordination in the rare-earth complex are described below:



Incorporation of [C₅H₅NC₁₆H₃₃][Eu(TTA)₄] into Si-MCM-41 and Three Surface-Silylated Si-MCM-41

(23) Feng, Y. Y.; Shen, Z. M.; Xin, S. J. *J. Rare Earths* **2000**, *18*, 3.

(24) Liu, C. J.; Li, S. G.; Pang, W. Q.; Che, C. M. *Chem. Commun.* **1997**, *6*, 65.

Samples. A total of 0.1 g of each mesoporous sample was mixed with 10 mg of [C₅H₅NC₁₆H₃₃][Eu(TTA)₄] in a 20 mL round-bottomed flask, and then 10 mL of chloroform was added with stirring. The mixture was continuously stirred for 48 h at room temperature followed by filtration and washing with chloroform until no red color was seen from the filtered solution with UV light. The solid was dried at room temperature.

Characterization. The crystal structures of the solid materials were examined by using a Rigaku D/MAX powder X-ray diffractometer with a Cu K α X-ray source ($\lambda = 0.15406$ nm). The pore-size distribution was measured by using the standard BJH method. The sample was first heated to 110 °C under a vacuum of 10⁻⁴ Torr for 4 h and then cooled to liquid-nitrogen temperature (77 K). Excitation and emission spectra were collected on a Spex Fluorolog-2T2 fluorimeter with a 450 W Xe lamp as an excitation light source. The optical slits for excitation and emission were 5.0 and 1.5 mm, respectively. The lifetime measurements of Eu³⁺ in the rare-earth complex were performed on a Spex 1934D phosphorimeter. Solid-state diffuse reflectance measurements were carried out on a ZF-1 photospectrometer. XPS analysis was conducted on an ESCLAB Mark II instrument with an Al K α light source. Measurements of the UV stability of the rare-earth complex in Si-MCM-41 and surface-modified Si-MCM-41 were made by using a 30 W high-pressure mercury lamp. The sample-to-lamp distance was set to 14 cm. Elemental analysis was done by using a Plasma-Spec (I) ICP-AES instrument. Solid-state ²⁹Si MAS NMR spectroscopic studies were carried out on a Unity-400 NMR spectrometer operating at 79.45 MHz. The spinning speed was 4K, and the recycle delay time was 1 s.

Results and Discussion

Surface Silylation. Figure 1 gives the ²⁹Si MAS NMR spectra of Si-MCM-41 and three surface silylated Si-MCM-41 samples. The bands labeled Q², Q³, and Q⁴ in Figure 1a correspond respectively to (OH)₂Si(OSi)₂, (OH)Si(OSi)₃, and Si(OSi)₄.²⁸ After silylation with these silylating agents, the relative intensities of the bands in the spectra are changed dramatically, indicating that silylation occurs during the treatment. The band assigned to Si(OSi)₄ increases in intensity and becomes dominant (see Figure 1b-d). From the figures it is clear that all three kinds of silylating agents are grafted onto the surface of Si-MCM-41 via reactions with OH groups on the channel wall. The reactions can be described as

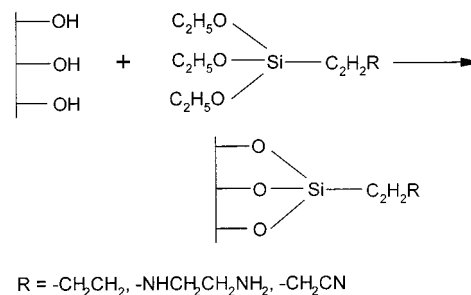


Table 1 summarizes the data of chemical shifts and deconvoluted band intensities. Comparing the relative intensities of the silylated materials with that of the starting Si-MCM-41 shows that more than 50% of the Si-OH groups on the surface are silylated.

(25) Zhang, J. Y.; Luz, Z.; Goldfarb, D. *J. Phys. Chem., B* **1997**, *101*, 7087.

(26) Melby, L. R.; Rose, N. J.; Abramson, E.; Caris, J. C. *J. Am. Chem. Soc.* **1964**, *86*, 5117.

(27) Bauer, H.; Blanc, J.; Ross, D. L. *J. Am. Chem. Soc.* **1964**, *86*, 5125.

(28) Zhao, X. S.; Lu, G. Q. *J. Phys. Chem., B* **1998**, *102*, 1556.

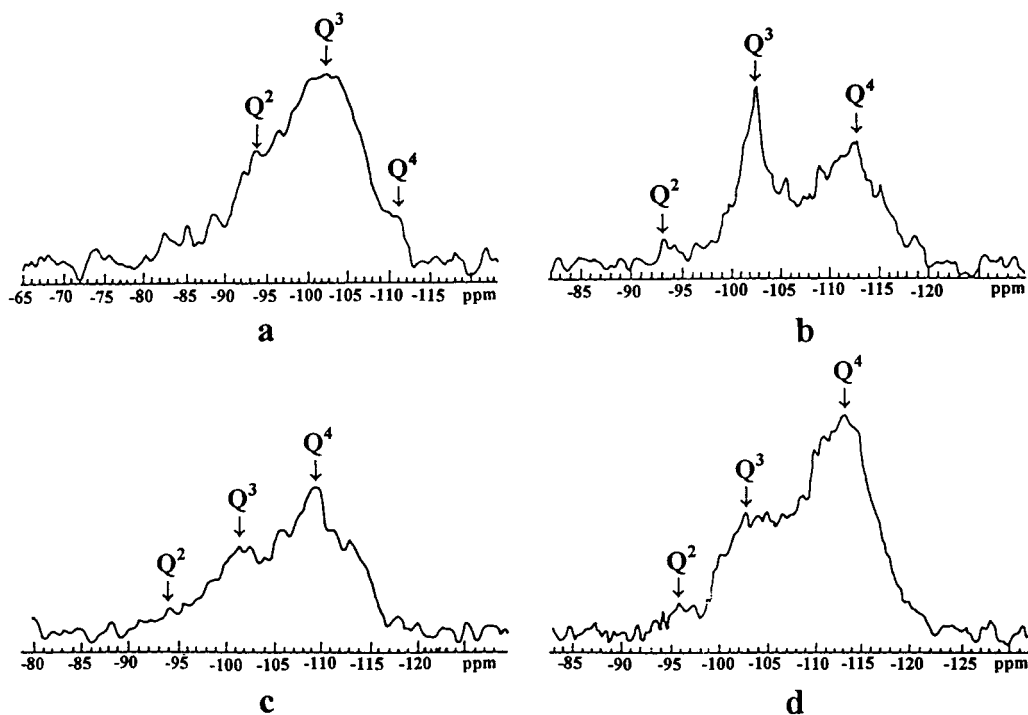


Figure 1. ²⁹Si MAS NMR spectra of (a) Si-MCM-41, (b) NSED-Si-MCM-41, (c) APTES-Si-MCM-41, and (d) TSBT-Si-MCM-41.

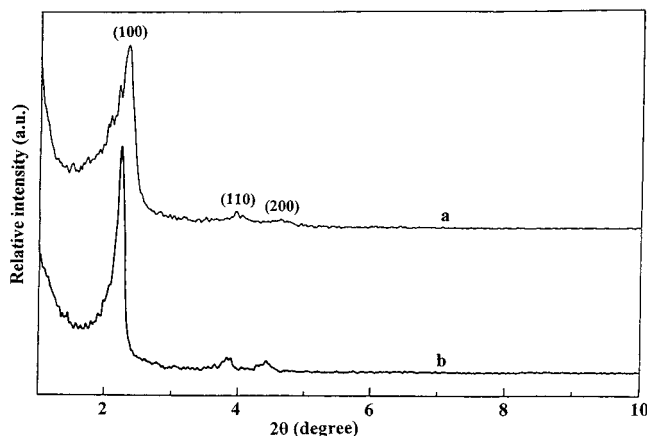


Figure 2. Powder XRD patterns of APTES-Si-MCM-41 samples with (a) and without (b) incorporated Eu(TTA)₄⁻ complex.

Table 1. ²⁹Si MAS NMR Data of Si-MCM-41 and Silylated Si-MCM-41 Samples

sample	chemical shift (ppm)			% intensity		
	Q ²	Q ³	Q ⁴	Q ²	Q ³	Q ⁴
Si-MCM-41	-94	-102	-113	26.9	44.8	21.5
NSED-Si-MCM-41	-94	-102	-113	3.6	36.2	60.2
APTES-Si-MCM-41	-94	-101	-110	4.2	31.1	64.7
TSBT-Si-MCM-41	-96	-103	-114	4.7	27.1	68.2

Eu(TTA)₄⁻ Incorporation and Interactions with Its Surroundings. Figure 2 gives the powder XRD patterns of APTES-modified Si-MCM-41 before (Figure 2b) and after (Figure 2a) incorporation of [C₅H₅NC₁₆H₃₃]-[Eu(TTA)₄]. Comparing the XRD patterns clearly shows that the incorporation of [C₅H₅NC₁₆H₃₃][Eu(TTA)₄] into the channels does not affect the Si-MCM-41 structure. Similar results were also obtained for NSED- and TSBT-modified Si-MCM-41 samples (not shown). The lack of diffraction peaks due to the incorporated rare-earth

complexes in the powder XRD patterns indicates that the complexes are highly dispersed in the mesoporous channels.

UV-vis diffuse reflectance spectra of the rare-earth complex containing silylated Si-MCM-41 materials together with the rare-earth complex and the starting Si-MCM-41 are given in Figure 3. The starting Si-MCM-41 does not have characteristic absorption bands in this entire spectral region (Figure 3a). Similar spectral characteristics are also observed for the three modified Si-MCM-41 samples (not shown). The rare-earth complex itself has absorption bands at 275, 331, and 465 nm (Figure 3c). The APTES-modified Si-MCM-41 with the incorporated rare-earth complex has absorption bands at 268, 328, 394, and 406 nm (Figure 3d). Compared to the pure complex, the major bands of the rare-earth complex are shifted toward shorter wavelengths. A similar phenomenon was also observed for the other modified Si-MCM-41 materials. Table 2 summarizes the absorption bands for all samples. The shifts of the bands compared to that of the rare-earth complex confirm that the rare-earth complex is incorporated into the Si-MCM-41 channels.²⁴

Silylation of the internal wall surface of Si-MCM-41 changes the chemical environment inside the channels. When the rare-earth complex was incorporated, interactions of the ligands of the rare-earth complex with their local chemical environment changed the symmetry of the Eu³⁺ complex. Because of this interaction, the polarity of the surroundings of the rare-earth ion was increased, as is evidenced by the shifts of the absorption bands toward higher energy (shorter wavelength) in the UV-vis spectra given above. The strength of the interaction can be evaluated by using the Lippert equation:²⁹

$$hc\Delta\nu = 2\Delta f(\mu^* - \mu)^2/a^3$$

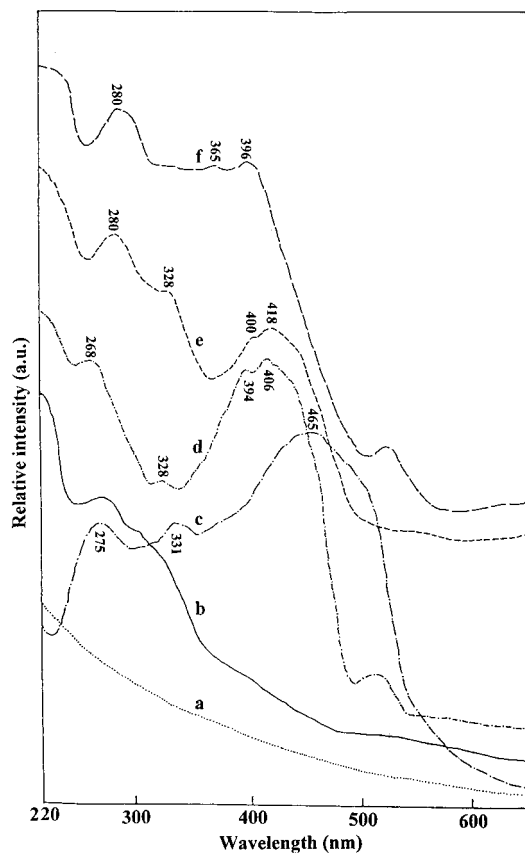


Figure 3. UV-vis absorption spectra of Si-MCM-41 (a), $\text{Eu}(\text{TTA})_4^-$ complex containing Si-MCM-41 (b), the pure $\text{Eu}(\text{TTA})_4^-$ complex (c), $\text{Eu}(\text{TTA})_4^-$ complex containing APTES-Si-MCM-41 (d), $\text{Eu}(\text{TTA})_4^-$ complex containing NSED-Si-MCM-41 (e), and $\text{Eu}(\text{TTA})_4^-$ complex containing TSBT-Si-MCM-41 (f).

Table 2. UV-Vis Absorption Spectroscopic Data of the Rare-Earth Complex in the Surface-Modified Si-MCM-41 Materials

sample	absorption (nm)		
$\text{Eu}(\text{TTA})_4^-$	275	331	465
NSED-Si-MCM-41	280	328	400
APTES-Si-MCM-41	268	328	394
TSBT-Si-MCM-41	280	365	396

Here f is the polarizability of the ligand molecule, h is the Planck constant, c is the light velocity, a is the diameter of the channel of molecular sieve, μ^* and μ are dipole moments of the excited and ground states of the Eu^{3+} ion, respectively, and $\Delta\nu$ is the frequency difference of the absorption band of the ligand. When the rare-earth complex is introduced, interactions of the complex with the wall of the molecular sieve result in an increase in the polarizability of the complex; i.e., f is increased and $\Delta f > 0$. Therefore, the frequency difference, $\Delta\nu$, of the absorption bands of the rare-earth complex before and after being intercalated in the channel is >0 . According to the band shift, it is clear that the strength of the interactions between the rare-earth complex and its surroundings increases in the order of $\text{TSBT} < \text{APTES} < \text{NSED}$. For unmodified Si-MCM-41, because of the low concentration of the rare-earth complex ($\sim 0.24\%$) incorporated, the absorption bands are very

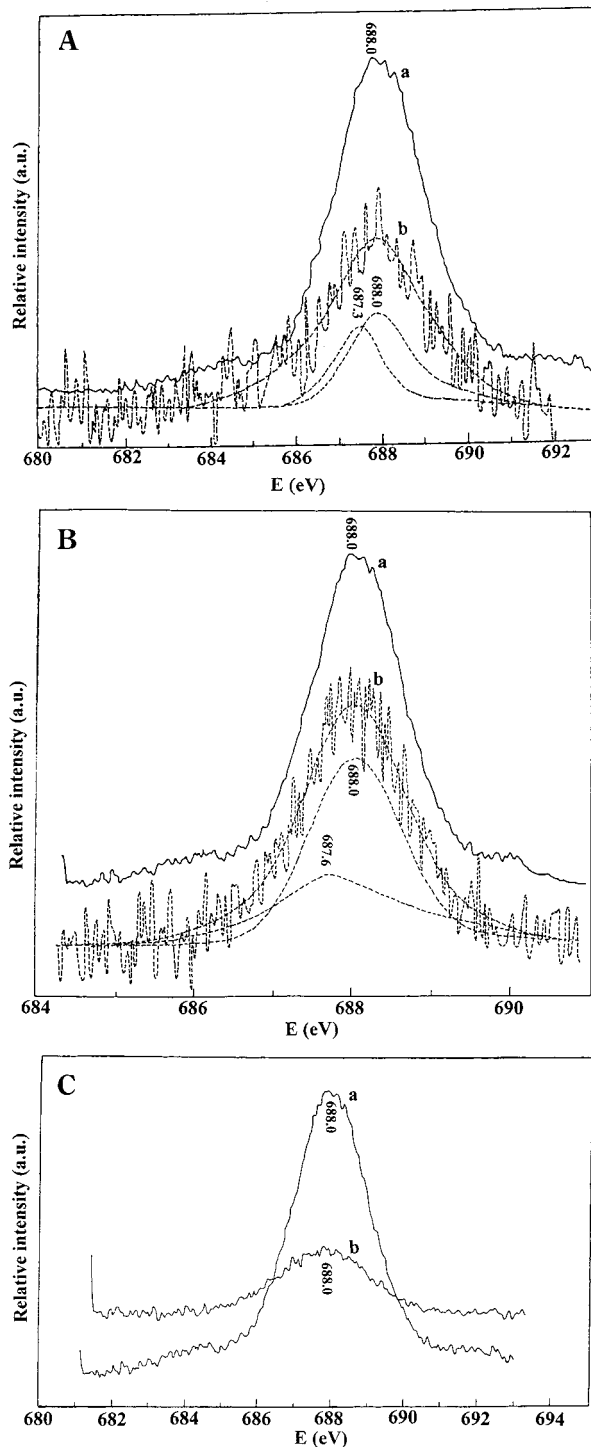


Figure 4. (A) XPS spectra of F 1s of the $\text{Eu}(\text{TTA})_4^-$ complex (a) and in NSED-Si-MCM-41 (b). (B) XPS spectra of F 1s of the $\text{Eu}(\text{TTA})_4^-$ complex (a) and in APTES-Si-MCM-41 (b). (C) XPS spectra of F 1s of the $\text{Eu}(\text{TTA})_4^-$ complex (a) and in TSBT-Si-MCM-41 (b).

weak, as seen from its UV-vis spectrum (see Figure 3b).

Figure 4 gives binding energies of the rare-earth complex in these materials. The F 1s electron binding energy of the pure rare-earth complex is 688.0 eV, while that of the rare-earth complex located in NSED-Si-MCM-41 has two different binding energies, 688.0 and 687.3 eV (see Figure 4A), respectively. The binding energy of the latter is 0.7 eV smaller than that of the pure rare-earth complex. Similar to NSED-Si-MCM-

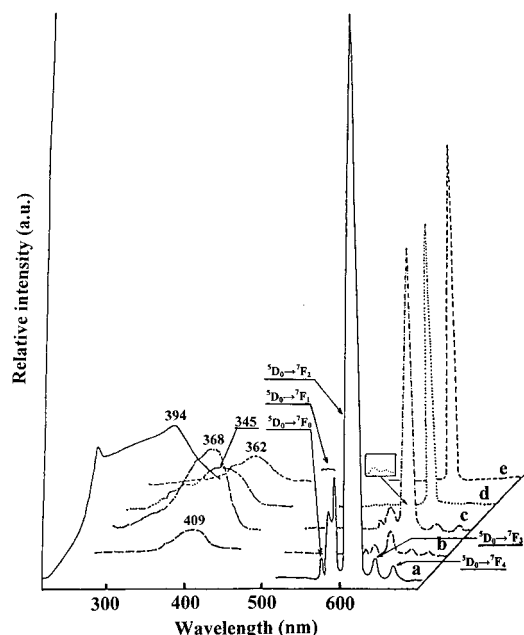


Figure 5. Excitation and emission spectra (the excitation spectra are monitored at 612 nm and the emission spectra with excitation at their maximum absorption band position, all of the samples tested are solid, and the test temperature is 293 K) of Eu(TTA)₄⁻ complex (a), Eu(TTA)₄⁻ complex containing Si-MCM-41 (b), Eu(TTA)₄⁻ complex containing TBST-Si-MCM-41 (c), Eu(TTA)₄⁻ complex containing APTES-Si-MCM-41 (d), and Eu(TTA)₄⁻ complex containing NSED-Si-MCM-41 (e).

41, the F atom in APTES-Si-MCM-41 also exists in two forms with 1s electron binding energies of 688.0 and 687.6 eV (Figure 4B). The difference in binding energy between these two forms in this sample is 0.4 eV. In contrast to these observations, the rare-earth complex in TBST-Si-MCM-41 has only one form of the F atom with a binding energy of 688.0 eV (Figure 4C). From these binding energy differences, it is understood that the interactions between the rare-earth complex and its surroundings occur via the F atom of the complex and the hydrogen atom on the -NH₂ group of the silylation agents that are grafted on the surface of Si-MCM-41. The nature of the interactions is hydrogen-bonding, and the strength of the interaction follows the order NSED > APTES > TBST. In the latter case, there are almost no hydrogen-bonding interactions owing to absence of H in the periphery of the molecule. This sequence is consistent with the band blue shift obtained from the above-mentioned UV-vis spectroscopic studies. In the starting Si-MCM-41, no F 1s is observed because of the low concentration of the rare-earth complex incorporated.

N 1s XPS studies of these samples show no binding energy shifts for both N atoms in the rare-earth complex and silylation agents, suggesting that after incorporation of the rare-earth complex into the silylated Si-MCM-41 channels no other chemical bonding occurs on the N atoms.

Photophysical Properties. Figure 5 gives excitation and emission spectra of the rare-earth complex in these surface-modified Si-MCM-41 samples. In Figure 5, the left spectra are excitation spectra monitored at 612 nm and the right spectra are emission spectra with excitation at their maximum absorption band position.

For the pure rare-earth complex (Figure 5a), the maximum absorption is around 394 nm and the emission spectrum has five bands at 577, 589, 612, 650, and 705 nm. The emission bands are associated with ⁵D₀ → ⁷F₀, ⁵D₀ → ⁷F₁, ⁵D₀ → ⁷F₂, ⁵D₀ → ⁷F₃, and ⁵D₀ → ⁷F₄, respectively, where ⁵D₀ → ⁷F_{1,3} are magnetic-dipolar transitions and insensitive to their local environment and ⁵D₀ → ⁷F_{0,2,4} are electric-dipolar transitions and sensitive to their local environment. When the interactions of the rare-earth complex with its local chemical environment are stronger, the complex becomes more nonsymmetric and the intensity of the electric-dipolar transitions becomes more intense. Figure 5c is the excitation and emission spectra of the rare-earth complex incorporated in the TBST-Si-MCM-41. The maximum absorption was found from the excitation spectrum to be at 368 nm, while the emission spectrum has five bands and is the same as that of the pure rare-earth complex. These spectral features reflect the weak interactions between the complex and the wall of the channel. Figure 5d gives the excitation and emission spectra of the same complex in APTES-Si-MCM-41. The maximum absorption is at 345 nm and the five emission bands are similar to those of the pure complex in the band position, but the intensities of the bands at 577, 589, 650, and 705 nm are greatly depressed. The ⁵D₀ → ⁷F₂ transition band at 612 nm is still strong. Figure 5e shows the excitation and emission spectra of the rare-earth complex located in NSED-Si-MCM-41. The maximum absorption is at 362 nm, and the emission bands all disappeared except for the ⁵D₀ → ⁷F₂ transition band at 612 nm. The ⁵D₀ → ⁷F₂/⁵D₀ → ⁷F₁ band intensity ratios for the three modified Si-MCM-41's, the rare-earth complex, and the starting Si-MCM-41 are ∞ (NSED), 103.7 (APTES), 13.8 (TBST), 3.6, and 5.5, respectively. The ⁵D₀ → ⁷F₂/⁵D₀ → ⁷F₁ band intensity ratio increases with the order TBST < APTES < NSED. This change reflects the increase of the ⁵D₀ → ⁷F₂ emission band intensity and the decrease of the other emission bands due to the increase in electric-dipolar interactions.

The changes in photophysical properties of these samples can be rationalized on the basis of the pore size of the silylated materials. The pore-size measurements of these materials show that after Si-MCM-41 was modified with two -NH₂ (NSED), -NH₂ (APTES), and -CN (TSBT), the pore size of Si-MCM-41 decreases from 2.9 nm to 1.42, 2.14, and 2.38 nm, respectively. Compared to the size of the rare-earth complex [C₅H₅NC₁₆H₃₃][Eu(TTA)₄],³⁰ 1.2 nm, the pore size of the NSED-Si-MCM-41, 1.42 nm, is just about a large enough size for the molecule to penetrate. Therefore, the F atoms on the rare-earth complex can bond with the hydrogen atoms on both -NH₂ and =NH groups of the silylation agent molecules grafted on any side of the channel wall (see the XPS results given above). In this case, the maximum interactions are achieved via interactions of each silylation agent molecule with two TTA ligands and all four TTA ligands in the rare-earth complex hydrogen bonding to the silylation agent (see Figure 6a). Because of the hydrogen-bonding interactions, the symmetry of the rare-earth molecule is no

(30) Huang, C. H. *Rare Earth Complexes*; Science Press: Beijing, 1997.

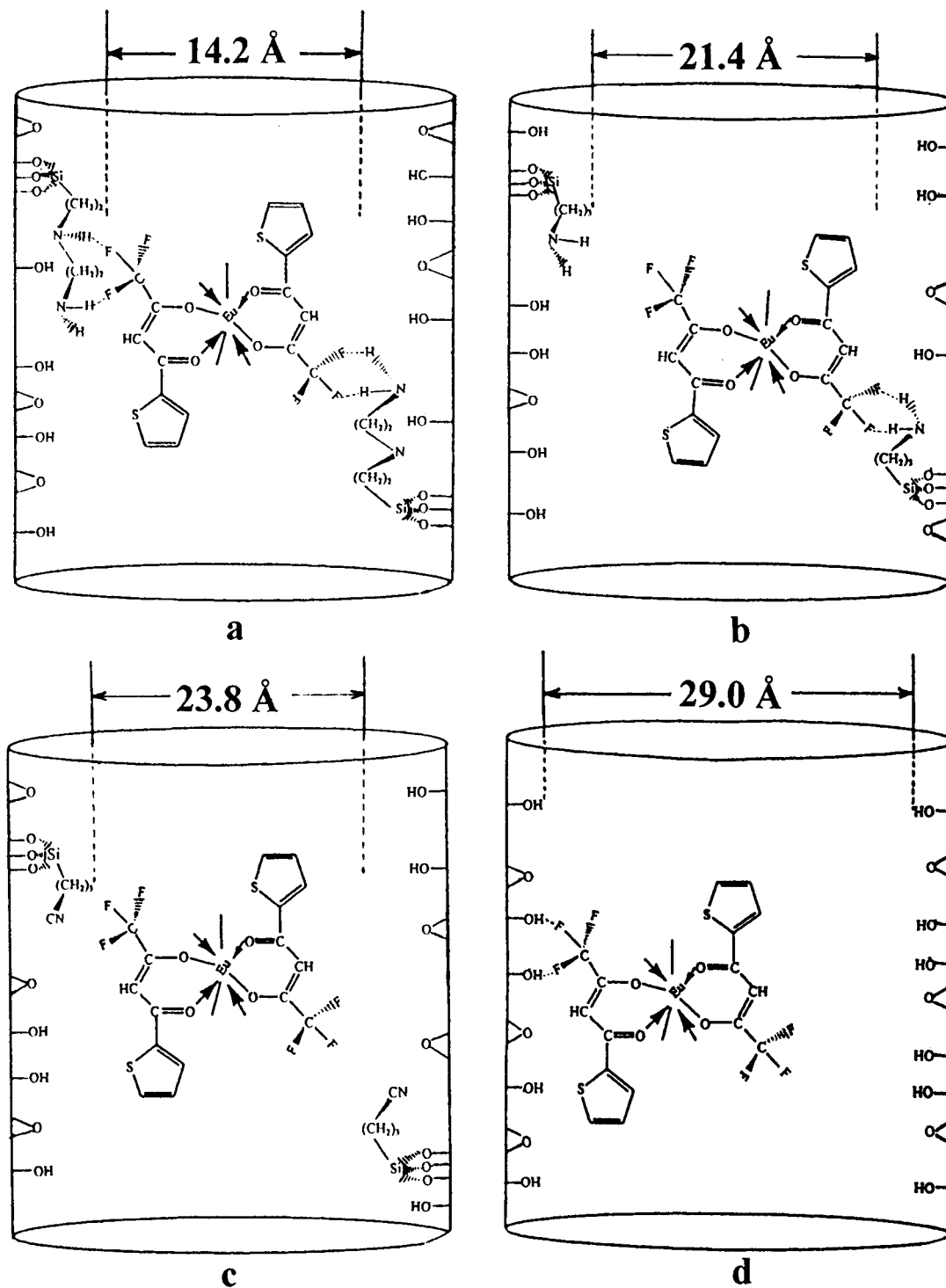


Figure 6. Schematic drawing of the $\text{Eu}(\text{TTA})_4^-$ complex in NSED-Si-MCM-41 (a), APTES-Si-MCM-41 (b), TSBT-Si-MCM-41 (c), and Si-MCM-41 (d).

longer held, leading to a great enhancement of the electric-dipolar $^5\text{D}_0 \rightarrow ^7\text{F}_{0,2,4}$ transitions and depression of the magnetic-dipolar $^5\text{D}_0 \rightarrow ^7\text{F}_{1,3,5}$ transitions. Because of the much smaller increase for the $^5\text{D}_0 \rightarrow ^7\text{F}_{0,4}$ transitions compared to the $^5\text{D}_0 \rightarrow ^7\text{F}_2$ transition, only the $^5\text{D}_0 \rightarrow ^7\text{F}_2$ transition is seen clearly in the spectrum. As discussed above, the symmetry of the rare-earth complex is changed from C_2 to D_4 after it was encapsulated into the channels of NSED-Si-MCM-41; the change of the emission spectrum of the rare-earth ion can be regarded as one of the best probes of the molecular structure.²⁷

For APTES-Si-MCM-41, the pore size is 2.14 nm, larger than the size of the rare-earth complex (1.2 nm). The F atoms in the rare-earth complex can only hydrogen bond with one single $-\text{NH}_2$ of the silylation agent molecule on one side of the channel wall. For this reason, the interactions are much smaller compared to the system interacting with both $-\text{NH}_2$ and $=\text{NH}$ groups (Figure 6b). Accordingly, the distortion of the symmetry of the $[\text{C}_5\text{H}_5\text{NC}_{16}\text{H}_{33}][\text{Eu}(\text{TTA})_4]$ molecule is less severe. For TSBT-Si-MCM-41, because the pore size (2.38 nm) is much larger than the size of the rare-earth complex and also there is only a $-\text{CN}$ group on

the molecule with no H, hydrogen-bonding interactions are not possible and therefore little distortion is observed (Figure 6c). The photophysical properties of the rare-earth complex in this sample are very similar to that of the pure rare-earth complex.

The strength of interactions between the rare-earth complex and silylation agent can also be seen from the amount of the rare-earth complex incorporated into these materials. The content of the rare-earth complex in the final products, obtained from chemical analysis, is 6.61% in NSED-Si-MCM-41, 1.84% in APTES-Si-MCM-41, 1.83% in TSBT-Si-MCM-41, and 0.42% in Si-MCM-41. This shows that the interaction between the rare-earth complex and NSED-MCM-41 is the strongest and the interaction between the rare-earth complex and the unmodified Si-MCM-41 is the weakest in these materials.

Lifetime measurements of Eu³⁺ in the Eu(TTA)₄ complex in these materials also provide further support for the conclusion about the interactions of the complex with its surroundings. The different strengths of hydrogen bonding in these modified Si-MCM-41 systems make the strengths of the molecular vibration and relaxation time different. The stronger the hydrogen-bonding interactions, the slower the vibration of the Eu(TTA)₄⁻ complex molecule and the longer the electron relaxation time and, as a consequence, the longer the emission lifetime. The lifetimes of the excited rare-earth complex in these samples are 0.84 ms for the pure complex, 2.18 ms for NSED-Si-MCM-41, 2.64 ms for APTES-Si-MCM-41, 0.74 ms for TSBT-Si-MCM-41, and 0.51 ms for Si-MCM-41. Compared to the pure complex (0.84 ms), the lifetimes for the modified Si-MCM-41 follow the sequence of interaction strength. The shortening of the lifetime in the starting Si-MCM-41 (0.51 ms) is due to the interactions of the complex with the OH groups on the channel wall.

Stability of the Rare-Earth Complex under UV Irradiation. It is well-known that instability of rare-earth complexes under UV irradiation is one of the problems in their application. The stability depends on the vibrations of the complex after absorbing light. The more intense the vibrations, the faster the decomposition of the complex. For the NSED- and APTES-Si-MCM-41 materials, strong hydrogen-bonding interactions of the rare-earth complex with the NSED and APTES molecules significantly limit the vibrations of the rare-earth complex. As a consequence, the decomposition of the rare-earth complex is slowed significantly. Figure 7 gives the decay curves of the ⁵D₀ → ⁷F₂ emission band as a function of irradiation time (UV lamp power *P* = 30 W, and the distance between the lamp and the sample is 14 cm), and Table 3 summarizes the half-life data of the photodecomposition of these samples obtained from these curves.³¹ From the figure and the table, it is clear that compared to the pure rare-earth complex the incorporated Eu(TTA)₄ complex in these modified Si-MCM-41 materials is much more

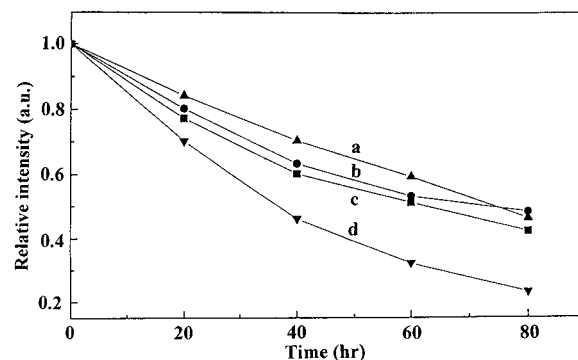


Figure 7. Changes of emission intensities of the Eu(TTA)₄ complex in APTES-Si-MCM-41 (a), NSED-Si-MCM-41 (b), TSBT-Si-MCM-41 (c), and Si-MCM-41 (d).

Table 3. Half-Life Data of Decomposition of Rare-Earth Complex in Si-MCM-41 and Surface-Modified Si-MCM-41

	sample			
	pure complex	TBST	APTES	NSED
half-life time (h)	36	64	73	75

stable. The half-life of decomposition follows the order of the hydrogen-bonding strength of the rare-earth complex with its surroundings.

Conclusions

We have successfully incorporated the rare-earth complex [C₅H₅NC₁₆H₃₃][Eu(TTA)₄] into surface-modified mesoporous molecular sieve Si-MCM-41. Characterization of the materials has shown that strong hydrogen-bonding interactions exist between the rare-earth complex and the silylating agent and the interaction strength follows the order of NSED > APTES > TSBT. The hydrogen-bonding interactions affect the emission properties of the rare-earth complex by distorting the rare-earth complex. This effect gradually changes the emission from multicolor to a single color. In the NSED-modified Si-MCM-41, the rare-earth complex only emits 612 nm light. The environments of the modified Si-MCM-41 also protect the rare-earth complex and prevent it from undergoing UV photodecomposition. The half-lifetime of the decomposition of the rare-earth complex in these materials under UV irradiation is almost double that of the pure complex. Compared to the pure complex, in the incorporated surface-modified Si-MCM-41 materials, the modified Si-MCM-41 provides a unique chemical environment for the rare-earth complex, and it is this special guest-host interaction that changes the photophysical properties of the rare-earth complex. The extension of the lifetime of the rare-earth complex in these modified Si-MCM-41 materials under UV irradiation can become a solution for the instability problem in applications.

Acknowledgment. We are grateful to the National Natural Science Foundation of China for financial support.

(31) Avnir, D.; Kaufman, V. R.; Reisfeld, R. *J. Non-Cryst. Solids* **1985**, *74*, 395.